A 180 nm-CMOS Asymmetric UWB-RFID Tag with Real-time Remote-monitored ECG-sensing

Jue Shen[1], Jia Mao[1], Geng Yang[1], Li Xie[1], Yi Feng[1], Majid Baghaei Nejad[2], Zhuo Zou[1],
Fredrik Jonsson[1], Hannu Tenhunen[1] and Lirong Zheng[1,3]

[1]*iPack Center, KTH-Royal Institute of Technology, Electrum 229, Stockholm, Sweden*
[2]*Electrical and Computer Engineering Department, Hakim Sabzevari University, Sabzevar, Iran*
[3]*School of Information Science and Technology, Fudan University, 200433, Shanghai, China*

Abstract: This paper proposes an asymmetric ultra-wideband - radio frequency identification (UWB-RFID) tag with electrocardiogram (ECG)-sensing capability for patients remote-monitoring in hospital environment. A UWB-RFID communication protocol is suggested for real-time transmission of undistorted ECG by interleaving ADC sampling and burst-mode UWB transmission. The proposed system shows a maximum accessing capability of 400 tags/second at 1.5 KHz ECG sampling rate with 10 Mbps UWB pulse rate. The tag consists of UHF-RFID receiver, UWB transmitter, ECG analog front-end, multi-input ADC and baseband circuitry integrated on two silicon dies. It was implemented by 6 mm^2-sized 180 nm CMOS technology. Electrodes for ECG-sensing are manufactured by inkjet-printing on polyimide substrate. Experiment results show that the tag transmits UWB pulses at 1 Mbps rate with 18 μW power. The printed electrodes conduct ECG waveform comparable to commercial electrodes.

1 INTRODUCTION

Wireless electrocardiogram (ECG) tags, enabling real-time remote-monitoring of ECG waveform for in-hospital patients, greatly reduce hospital manpower, increase response accuracy and improve patient comfort. As an example, for patients recovering from serious diseases, such tags facilitate them to do rehabilitation exercises and shorten recovering periods while ECG signals are continuously monitored at backend central server. However, typical solutions of ECG tags store data in large-sized memories and do not activate transmission unless certain pre-defined conditions are detected; or transmit ECG signal that is sampled below 1 KHz (Medtronic, 2014; Pantelakis et al., n.d.). As results, though tag complexity and power consumption are greatly decreased, these conditions significantly reduce detection accuracy and range of cardiac symptoms, unsuitable for hospital-targeted real-time remote-monitoring.

This paper proposes an ultra-wideband - radio frequency identification (UWB-RFID) tag with ECG-sensing for real-time remote-monitoring of in-hospital patients. ECG data of multiple patients are sampled at KHz rate and transmitted to backend server in real-time. It reduces buffer size for data storage and design complexity for data processing at the tag side. Among various item-level short-ranged wireless communications, ultra-high frequency RFID (UHF-RFID) has been verified as one most cost-power-effective method for multi-object data collection (Reinisch et al. 2011). UWB Impulse Radio (UWB-IR) which outputs ultra-short pulse and ultra-wide bandwidth supports Mbps data rate without significant increase in circuit power and implementation cost (Zheng et al., 2010).

Following of the paper is organized as: section 2 introduces system architecture and communication protocol of UWB-RFID tag. Section 3 discusses tag circuit and inkjet-printed ECG electrodes implementation. Section 4 demonstrates test results. Section 5 concludes and outlooks the work.

2 SYSTEM DESCRIPTION

2.1 System Architecture

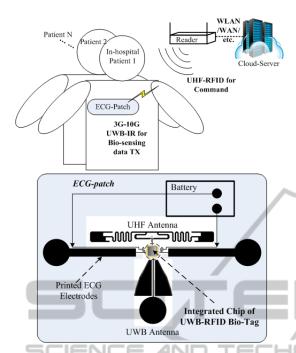System architecture of the tag is illustrated in Fig. 1.

Figure 1: System architecture of UWB-RFID bio-tag.

ECG data sampled at several KHz rate are transmitted to and processed at cloud server in real-time. Low communication power and high transmission data rate are hence the challenges of tag design. Especially in multi-tag accessing scenarios, uplink traffic from tags to reader is far more crowded than downlink from reader to tags.

Therefore, the tag integrates UHF-RFID for downlink reception because RFID network is star-structured, suitable for multi-tag accessing; and RFID receiver is non-coherent, suitable for low power tag. To the contrast, it integrates UWB-IR for uplink transmission because data rate is high and UWB-IR transmitter is digital-intensive, suitable for low-power real-time transmission. The asymmetric transceiver is much less complicated than transceiver for longer-ranged communications such as WLAN (wireless local area network), greatly reducing tag cost and increasing battery life time.

Such asymmetric radio links pay cost at the reader side which is area and power hungry. UWB-RFID reader works as gateway to relay the communications between tag and server as shown in Fig. 1. However for in-hospital applications, the number and allocation of readers are basically fixed and power consumption is not a fatal problem. Communication range of tag-to-reader layer is above 10 meters (Zheng et al., 2010).

Targeting future wearable ECG-patch, chip part of the tag is minimized by implementation in 180-nm CMOS process. Moreover, inkjet-printing technology is utilized to fabricate ECG electrodes on polyimide substrate based on noise characterization and impedance study of dry electrodes in (Xie et al., 2012). Battery is used to improve communication distance and performance stability.

2.2 UWB-RFID Communication Protocol for ECG Transmission

Fig. 2 illustrates the UWB-RFID communication protocol for ECG transmission in real-time. In general, ECG sampling and UWB transmission (TX) in burst mode are interleaved based on an improved frame-slotted-ALOHA protocol.
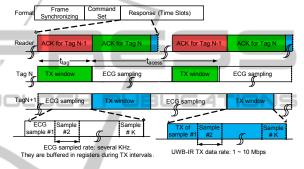

Figure 2: UWB-RFID protocol for real-time ECG TX.

Frame-slotted-ALOHA is a typical algorithm for anti-collision in multi-tag accessing. A frame represents an operation initiated by readers and is composed by three phases: start of frame (SOF), commands, and response. A frame time is divided into discrete time intervals, called slots. A tag randomly selects a slot number and responds to the reader. An acknowledgement (ACK) is sent from reader to a specific tag to ensure successful reception and to resolve collision. Collided tags retransmit in next frames. Such anti-collision protocol can be improved by pipelining reader ACK and tag TX to reduce slot length, optimizing frame size, and skipping idle slot, achieving simulated throughputs up to 2000 tags/s (Zhuo et al., 2007).

Real-time ECG TX makes use of the improved protocol as follows: ECG data are sampled and buffered during TX intervals of one tag, and the buffered data are completely transmitted in next TX window. To reduce complexity of tag register management, ECG sampling is temporarily disabled during UWB TX. Since UWB TX rate is much higher than ECG sampling rate, missing percentage of ECG data is very low. For an example of 3.75 ms UWB TX window, data missing percentage for ECG at 1.5 KHz sampling rate is 5.625%.

Tag UWB TX window is designed no shorter than reader ACK window to decrease TX gap and increase system efficiency. In optimized case, there is no time gap or no idle slot between consecutive tag TX windows. Therefore, the number of accessed tags per second is shown in expression 1, of which the related parameters are shown in table I. For ECG signals with 1.5 KHz sampling rate and 16-bit UWB data per sample, it offers approximate 400 tags/s accessing capability at 10 Mbps UWB-IR TX rate and 0 dB processing gain. However, in real case, tag selects TX slot in a frame randomly; moreover idle slots and tag collision cannot be eliminated. Thus, system throughput is dependent on trade-off of frame size and collision probability in proportional to N_{opt} (Zhuo et al., 2007).

Because UWB TX is aggressively duty-cycled in the protocol, average power consumption of UWB TX is much lower than active power as shown in expression 2.1 and 2.2 (Nejad et al., 2009), making real-time ECG TX feasible within tag power budget.

$$N_{opt} = \frac{f_{tx}}{K \cdot N_b \cdot PG \cdot f_{ECG}} \quad (1)$$

$$P_{active} = E_{pulse} \cdot f_{tx} \quad (2.1)$$

$$P_{avg} = P_{active} \cdot t_{tag} / t_{access} \quad (2.2)$$

Table 1: Parameters for UWB-RFID communication protocol and power consumption.

N_{opt}	Optimized number of accessed ECG-tags per second
K	ECG samples per TX window
f_{tx}	UWB-IR TX data rate (bps)
f_{ECG}	ECG sampling frequency (Hz)
N_b	bits per sample
PG	TX processing gain (pulse per bit)
E_{pulse}	circuit energy consumption per UWB pulse
t_{tag}	tag TX window length
t_{access}	averaged tag access period
P_{active}	active UWB TX power
P_{avg}	averaged UWB TX power

3 TAG IMPLEMENTATION

According to the system architecture in Fig. 1, tag diagram is illustrated in Fig. 3. Circuit blocks are implemented in two silicon dies, and are composed of UWB-IR transmitter, UHF-RFID receiver, power management unit (PMU), successive-approximation-register ADC (SAR-ADC), baseband (BB) circuitry and analog front-end (AFE) sensing ECG signals.
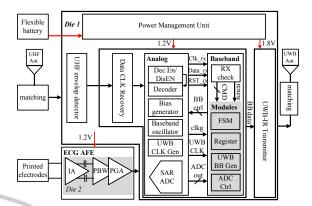

Figure 3: Tag implementation diagram.

Both UWB TX distance and power consumption are key consideration for bio-tag applications. Therefore supply voltage for UWB transmitter is kept 1.8 V while that for other blocks are reduced to 1.2 V. Thus, a power management unit (PMU) integrates two voltage regulators to generate the two supplies from a single battery voltage input. In the voltage regulator, feedback comparator establishes negative feedback to stabilize the output voltages.

Tag receives UHF-RFID commands that are modulated by amplitude shift keying and encoded by pulse interval (ASK-PIE) from reader. Modulation index is 90%. Low interval for data 0 is 6.25 µs and 18.75 µs for data 1. Reception (RX) block is composed of envelop detector, envelop recovery and data decoder. To reduce reception power, analog decoder is implemented by charging a capacitor when envelop is high. Sequential baseband block of RX check checks ID while shifting in the serially-decoded data, and generates a renew signal once the check is correct. The renew signal triggers the data to the baseband registers in this clock period.

3.1 Operation Flow

According to the communication protocol in section 2, UWB TX and ADC sampling are both controlled by reader. A renew signal marks the RX of a new reader command and the start of assigning configure registers. Data in configure registers enable/disable ADC sampling, and together with (pseudo number) PN counting, enable/disable UWB TX in random slots. Corresponding to the protocol in Fig. 2, ADC is also disabled when UWB TX is enabled; and UWB TX is also disabled when data buffered during TX interval are all read out and successfully received. Such operation flow is shown in Fig. 4. TX state and ADC sample state are interleaved in applications of real-time ECG remote-monitoring.
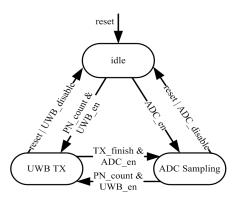
Figure 4: Operation flow.

3.2 Uwb Tx

AFE output of ECG signal is sampled and converted to 8-bit data by SAR-ADC at ADC clock rate. Data are continuously buffered until UWB TX is activated. When UWB TX is activated according to operation flow in Fig. 4, ID and ADC data are read out in serial by rising edge of UWB TX clock (UWB_CLK), and each bit are repeated by PG times. Rising edge of the output data triggers the UWB-IR transmitter. Transmitter NOR the rising edge and its delayed inverted result, and filters the output to UWB-shaped pulse (Mao et al., 2014).

Two clock domains are used. ADC clock is divided from global clock and the division ratio is received from reader command for different bio-applications. It is further gated by ADC enable signal to reduce power consumption. UWB TX clock are generated by down-scaling UHF carrier wave (CW) with harmonic injection locked divider (HILD) first and then with digital dividers according to commanded data rate (Mao et al., 2014).

3.3 Inkjet-Printed Electrodes and AFE

Inkjet-printed electrodes are fabricated by direct printing of NPS-JL (nano-particle silver inkjetable

low temperature ink from Harima Chemicals) with a 10 pL printhead on commercial polyimide (PI) foil (Kapton 500HN, DuPont) substrate. The substrate has advantages of smoother surface, less shrinking, and more stable chemical and moisture conductance. They are sintered at 145 °C for 1 hour (Xie et al., 2012).

Amplitude of ECG signals varies due to size, pair distance and contact impedance of the printed electrodes. Therefore, a variable-gain-bandwidth amplifier is implemented in AFE. The AFE consists of three amplifier stages, of which the first stage is differential instrument amplifier with common-mode feedback and the other stages are single-end amplifiers with programmable capacitor arrays at input and output ends for gain and bandwidth tuning. It outputs up to 49 dB gain from 0.35 Hz to 1.5 KHz at 2.76 µW power consumption (Yang et al., 2012).

4 EXPERIMENTAL RESULTS

Fig. 5 illustrates the silicon die photo of UWB-RFID tag with ECG-sensing. UWB-RFID tag die is shown in Fig. 5 (a). AFE for ECG is currently implemented in another die as shown in Fig. 5 (b). Most area-consuming parts are inductors of UWB transmitter and capacitors of SAR ADC in UWB-RFID die, as well as programming capacitors in AFE die. Both dies are implemented in UMC-180 nm CMOS technology process. UWB-RFID die is tested separately by inputting ADC with emulated amplified cardiac signals from signal generator (Agilent 33250A). In future design, both dies will be integrated in a single die and signal generator will be replaced with AFE output.

4.1 UHF-RFID Reception

Tags demodulate and decode UHF-RFID envelop to generate decoded data (Dec_out). Analog decoder is
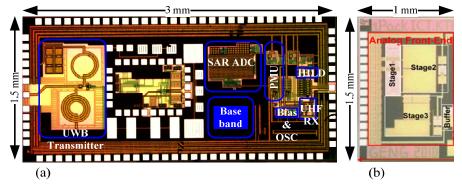

Figure 5: Silicon die photos of UWB-RFID tag (a) with ECG sensing (b).

conditionally enabled to save power consumption. As illustrated in Fig. 6, the decoder enable (Dec_enb) outputs high to disable decoding when a high envelop duration over 22 µs is detected and outputs low to enable it when a falling edge of RF envelop is detected.

Dec_out consists of four parts: starter, data command, tag ID, and ID checking. Data command includes configuration data such as UWB en/disable and bio-sensing en/disable. ID check validates one specific tag to be accessed. The time window of one reader command package lasts around 2.2 ms when RX data rate is 40 - 80 Kbps. According to the protocol in section 2, tag TX window is selected more than 2.2 ms to reduce time gaps between transmission slots of multiple tags. Thus, 3.75 ms is used as an example in the following UWB TX experimental results.
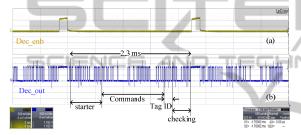

Figure 6: UHF-RFID command RX.

4.2 Real-time UWB-IR TX

Fig. 7 shows multiple transmission slots of one tag, demonstrating UWB TX interleaved with ECG samplings of one tag. UWB BB data and UWB TX pulse are illustrated in Fig. 7 (a) and (b). Corresponding to the protocol in Fig. 2, UWB-IR TX happens in the response phase. According to the reader command window length of 2.2 ms as demonstrated in Fig. 6, 3.75 ms of tag TX window is selected as an example. For an assumed multi-accessing scenario of 40 tags, the transmission interval is thus 146.25 ms and is left for the UWB TX of the other 39 ECG-tags in ideal case. ECG signal sampled by ADC at 1.5 KHz rate are buffered
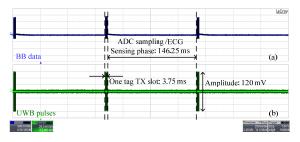

Figure 7: UWB TX interleaving with ADC sampling.

during the transmission intervals, and the number of buffered samples is around 219. They are transmitted together with tag ID in burst mode at 1 Mbps data rate in the next TX window.

Fig. 8 zooms in one tag TX slot of one ECG sample. UWB pulse rate is 1 Mbps (Fig. 8 (a)) and modulation is on-off-keying (OOK) (Fig. 8 (b)). As described in section 3, BB data is input to UWB-IR transmitter and triggers a pulse at its rising edge. Fig. 8 (c) illustrates the further zoomed-in result of one UWB pulse. Pulse shape is not optimized when chip output impedance is not matched to antenna impedance by matching network.
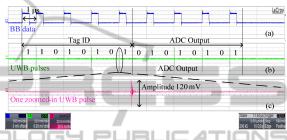

Figure 8: UWB TX of 1 ADC data @ 1 Mbps pulse rate.

Fig. 9 demonstrates the UWB pulses after impedance matching. Pulse Amplitude is increased to 1.02 V and duration decreased to 620 ps. UWB transmitter is measured to consume 18 µW when continuously transmitting pulses at 1 Mbps rate.
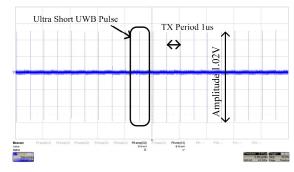

Figure 9: UWB pulses @ 1 Mbps pulse rate.

4.3 ECG by Inkjet-Printed Electrodes

Fig. 10 (a) shows ECG signals captured by inkjet-printed electrodes in Fig. 10 (b). Although the electrodes have different sizes and pair distances, the effects on electric parameters are compensated by variable-gain-bandwidth amplifier in AFE. The result is measured at AFE output separately. In future single-die solution, it will be input to ADC.
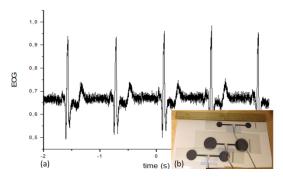
214

Figure 10: Measured ECG by inkjet-printed electrodes.

5 CONCLUSIONS AND OUTLOOKS

This paper proposes a UWB-RFID tag with ECG-sensing ability for low power and real-time patients remote-monitoring in hospital application scenarios. For undistorted ECG TX of multiple patients, burst-mode TX and ECG sampling are interleaved based on an improved frame-slotted-ALOHA protocol. It suggests a maximum accessing capability of 400 tags/s at 10 Mbps transmission data rate and 1.5 KHz sampling rate. UWB-IR transmitter is implemented to achieve Mbps data rate with low power consumption, whereas non-coherent UHF-RFID receiver is used for low-power tag accessing. The tag is implemented in two silicon dies manufactured by UMC-180nm-CMOS technology process. Total die area is 6 mm^2. Targeting future wearable ECG-patch, ECG electrodes are fabricated by inkjet-printing on polyimide substrate. Experimental results show that UWB-IR transmitter consumes 18 μW at 1 Mbps rate, corresponding to 18 pJ/pulse. AFE output of ECG signals captured by the printed electrodes is comparable to that by commercial electrodes.

To outlook this work: in current prototype, AFE is implemented in a separate die, yet it can be integrated with UWB-RFID tag in one single die. UWB and UHF communication are realized by conventional antenna, however flexible antenna can be used in the future with correspondent passive matching networks (Khaleel et al., 2012).

REFERENCES

Medtronic (2014). Introducing Seeq, mobile cardiac telemetry system. Retrieved October 10, 2014, from http://www.medtronicdiagnostics.com/wcm/groups/m dtcom_sg/@mdt/documents/documents/seeq-system-overview.pdf.

Pantelakis G., Leila S., Panu K., Damitha A., Matt A., Timothy G. C., Tor S. L. and Chris T., Development of an ultra-low power wireless Sensium platform providing personalized healthcare for chronic disease management. Retrieved October 10, 2014, from http://www3.imperial.ac.uk/pls/portallive/docs/1/3182 9696.PDF.

Reinisch H., Wiessflecker M., Gruber S., Unterassinger H., Hofer G., Klamminger M., Pribyl W. and Holweg G. (2011), A Multi-Frequency Passive Sensing Tag with On-Chip Temperature Sensor and Off-Chip Sensor Interface Using EPC HF and UHF RFID Technology. IEEE Journal of Solid-State Circuits, 46, 3075-3088.

Zheng Y.J., Diao S. X., Ang C.W., Gao Y., Choong F.-C., Chen, Z., Liu X., Wang Y.-S., Yuan X.-J. and Heng C.H. (2010), A 0.92/5.3nJ/b UWB Impulse Radio SoC for Communication and Localization. 2010 IEEE International Solid-State Circuits Conference Digest of Technical Papers (ISSCC), 230-231. doi: 10.1109/ISSCC.2010.5433934.

Xie L., Yang G., Mäntysalo M., Jonsson F. and Zheng L.-R. (2012), A System-on-Chip and Paper-Based Inkjet Printed Electrodes for a Hybrid Wearable Bio-Sensing System. 2012 Annual International Conference of the IEEE Engineering in Medicine and Biology Society (EMBC), 5026-5029. doi: 10.1109/EMBC.2012. 6347122.

Zhuo Z., Baghaei-Nejad M., Tenhunen H. and Zheng L.-R. (2007), An Efficient Passive RFID System for Ubiquitous Identification and Sensing using Impulse UWB Radio. Elektrotechnik und Informationstechnik, 124, 397-403.

Baghaei-Nejad M., Mendoza D. S., Zou Z., Radiom S., Gielen G., Li-Rong Z. and Tenhunen H. (2009), A Remote-Powered RFID Tag with 10Mb/s UWB Uplink and -18.5 dBm Sensitivity UHF Downlink in 0.18 um CMOS. IEEE International Solid-State Circuits Conference Digest of Technical Papers (ISSCC), 198-199,199a.

Mao J., Zou Z. and Zheng L.-R. (2014), A Sub-GHz UWB Transmitter with Wireless Clock Harvesting for RF-powered Applications. IEEE Transactions on Circuits and Systems II: Express Briefs, 61, 314-318.

Yang G., Xie L., Mäntysalo, M., Chen J., Tenhunen H. and Zheng L.-R. (2012), Bio-Patch Design and Implementation Based on a Low-Power System-on-Chip and Paper-Based Inkjet Printing Technology. IEEE Transactions on Information Technology in Biomedicine, 16, 1043-1050.

Khaleel, H.R., Al-Rizzo, H.M., Rucker, D.G. and Mohan, S. (2012), A Compact Polyimide-Based UWB Antenna for Flexible Electronics. IEEE Antennas and Wireless Propagation: Letters, 11, 564-567.